Communication

Development of Highly Sensitive Anti-Mouse CD39 Monoclonal Antibodies C39Mab-1 and C39Mab-2 for flow cytometry

Hiroyuki Suzuki [1], Yuma Kudo [1], Mayuki Tawara [1], Nohara Goto [1], Kenichiro Ishikawa [1], Tsunenori Ouchida [1], Tomohiro Tanaka [1], Teizo Asano [1], Takuro Nakamura [1], Miyuki Yanaka [1], Mika K. Kaneko [1] and Yukinari Kato [1,*]

[1] Department of Antibody Drug Development, Tohoku University Graduate School of Medicine, 2-1 Seiryo-machi, Aoba-ku, Sendai, Miyagi 980-8575, Japan; hiroyuki.suzuki.b4@tohoku.ac.jp (H.S.); kudo.yuma.p4@dc.tohoku.ac.jp (Y.Kudo); tawara.mayuki.p8@dc.tohoku.ac.jp (M.T.); s1930550@s.tsukuba.ac.jp (N.G.); ken.ishikawa.r3@dc.tohoku.ac.jp (K.I.); tsunenori.ouchida.d5@tohoku.ac.jp (T.O.); tomohiro.tanaka.b5@tohoku.ac.jp (T.T.); teizo.asano.a7@tohoku.ac.jp (T.A.); takuron@med.tohoku.ac.jp (T.N.); miyuki.yanaka.c5@tohoku.ac.jp (M.Y.); k.mika@med.tohoku.ac.jp (M.K.K.)

* Correspondence: yukinari.kato.e6@tohoku.ac.jp (Y.Kato.); Tel.: +81-22-717-8207

Abstract: CD39 is involved in adenosine metabolism through conversion of extracellular ATP to adenosine. Because extracellular adenosine plays a critical role in the immune suppression of tumor microenvironment, the inhibition of CD39 activity by monoclonal antibodies (mAbs) is one of the important strategies for tumor therapy. In this study, we developed specific and sensitive mAbs for mouse CD39 (mCD39) using the Cell-Based Immunization and Screening (CBIS) method. The established anti-mCD39 mAbs, which were established by the CBIS method including C39Mab-1 (rat IgG_{2a}, kappa) and C39Mab-2 (rat IgG_{2a}, lambda), reacted with not only mCD39-overexpressed Chinese hamster ovary-K1 (CHO/mCD39) but also endogenously mCD39-expressed cell lines, such as L1210 (mouse lymphocytic leukemia) and J774-1 (mouse macrophage-like) cell lines through flow cytometry. Kinetic analyses using flow cytometry indicated that the dissociation constant (K_D) of C39Mab-1 and C39Mab-2 for CHO/mCD39 was 7.3×10^{-9} M and 5.5×10^{-9} M, respectively. K_D of C39Mab-1 and C39Mab-2 for L1210 was 3.3×10^{-9} M and 3.6×10^{-10} M, respectively. Furthermore, C39Mab-1 could detect the lysate of CHO/mCD39 by western blot analysis. These results indicate that C39Mab-1 and C39Mab-2 are useful for the detection of mCD39 in many functional studies.

Keywords: mouse CD39; monoclonal antibody; the Cell-Based Immunization and Screening; CBIS

1. Introduction

Extracellular adenosine (eADO), which is generated by the hydrolysis of extracellular ATP (eATP), mediates immunosuppressive tumor microenvironment (TME) [1]. High concentration of eATP can be found in solid tumors due to not only passive release of cell death, but also active secretion by tumor cells and other subsets in the TME [2]. Following the release of eATP, CD39 (ectonucleoside triphosphate diphosphohydrolase 1; encoded by *ENTPD1*) hydrolyzes eATP to ADP and AMP. Then, another rate-limiting ectoenzyme, CD73 (5′-nucleotidase; encoded by NT5E), dephosphorylates AMP into adenosine [3].

A growing body of evidence suggests that adenosine-mediated immunosuppression is a critical mechanism of tumor immune evasion. Various tumors showed the elevated expression of CD39, which promotes the local accumulation of adenosine surrounding tumors [4]. The adenosine-mediated immunosuppressive effect functions via four G protein-coupled type 1 purinergic (P1) receptors, A_1, A_{2A}, A_{2B}, and A_3 are expressed on immune cells [5]. Among four P1 receptors, the A_{2A} and A_{2B} are G_s-coupled receptors and trigger intracellular cAMP accumulation. The cAMP signaling mediates immunosuppression through the activation of effectors including protein kinase A [6].

 doi:10.20944/preprints202304.0032.v1

Sitkovsky's group first reported the immunosuppressive effect of A_{2A} receptor *in vivo* [7]. Inflammatory stimuli that caused minimal tissue damage in wild-type mice were sufficient to induce extensive tissue damage, more prolonged and higher levels of pro-inflammatory cytokines, and individual death in mice lacking the A_{2A} receptor [7]. The group also showed genetic evidence of the importance of the A_{2A} receptor in tumor immunity [8]. These findings impact on antitumor immunity by CD39–adenosine–A_2 receptor axis and several landmark studies have developed the multiple strategies targeting adenosine metabolism [3,9].

The development of anti-CD39 monoclonal antibodies (mAbs) is one of the strategies to modulate the adenosine metabolism. A preclinical study revealed that an anti-mouse CD39 (mCD39) mAb (clone B66), which can inhibit mCD39 activity *in vitro*, exhibited the antitumor effect in syngeneic models by the monotherapy and combination therapy with the PD-1 blockade [10]. This study also showed that B66 triggers an eATP–P2X7–inflammasome–IL-18 pathway that promotes tumor immunity, and overcomes anti-PD-1 resistance [10]. The anti-human CD39 mAbs (clones TTX-030, IPH5201, and SRF-617) were designed to inhibit CD39 enzymatic activity via allosteric inhibition and minimize Fc receptor-mediated engagement to avoid the side effect [10,11]. These mAbs have entered into clinical trials for solid tumors with combination of chemotherapeutic agents or immune checkpoint inhibitors [3].

The Cell-Based Immunization and Screening (CBIS) method includes the immunization of antigen-overexpressing cells and the high-throughput hybridoma screening using flow cytometry. Using the CBIS method, we have developed mAbs against membrane proteins, including CD19 [12], CD20 [13,14], CD133 [15], EpCAM [16,17], HER2 [18], HER3 [19], KLRG1 [20], TIGIT [21], TROP2 [22,23], programmed cell death ligand 1 (PD-L1) [24], podoplanin [25-36], CD44 [37,38], mouse CCR3 [39], mouse CCR8 [40], and human CCR9 [41] mAbs.

In this study, novel anti-mCD39 mAbs were developed by the CBIS method. We further evaluated its applications, including flow cytometry and western blot analyses.

2. Materials and methods

2.1. Preparation of cell lines

P3X63Ag8U.1 (P3U1), LN229, and Chinese hamster ovary (CHO)-K1 cells were obtained from the American Type Culture Collection (Manassas, VA). J774-1 (mouse macrophage-like) and L1210 (mouse lymphocytic leukemia) cells were obtained from the Cell Resource Center for Biomedical Research Institute of Development, Aging and Cancer Tohoku University (Miyagi, Japan).

The synthesized DNA (Eurofins Genomics KK) encoding mCD39 (Accession No.: NM_ 009848) was subcloned into a pCAGzeo_nPA-cRAPMAP vector. The amino acid sequences of the tag system were as follows: PA tag [42-44], 12 amino acids (GVAMPGAEDDVV); RAP tag [45,46], 12 amino acids (DMVNPGLEDRIE); and MAP tag [47,48], 12 amino acids (GDGMVPPGIEDK). The PA tag can be detected by an anti-human podoplanin mAb (clone NZ-1) [42-44,49-61]. Then, the mCD39 plasmid was transfected into CHO-K1 and LN229 cells, as described previously [39].

Roswell Park Memorial Institute (RPMI)-1640 medium (Nacalai Tesque, Inc., Kyoto, Japan) were used to culture CHO-K1, mCD39-overexpressed CHO-K1 (CHO/mCD39), P3U1, L1210, and J774-1 cells. Dulbecco's Modified Eagle Medium (DMEM) (Nacalai Tesque, Inc.) were used to culture LN229 and mCD39-overexpressed LN229 (LN229/mCD39). These media were supplemented with 10% FBS, 100 U/mL of penicillin, 100 μg/mL streptomycin, and 0.25 μg/mL amphotericin B.

All cells were grown in a humidified incubator at 37°C, at an atmosphere of 5% CO_2 and 95% air.

2.2. Antibodies

 doi:10.20944/preprints202304.0032.v1

An anti-mCD39 mAb (clone 5F2, mouse IgG_1, kappa) was purchased from BioLegend (San Diego, CA). Alexa Fluor 488-conjugated anti-rat IgG and Alexa Fluor 488-conjugated anti-mouse IgG secondary Abs were purchased from Cell Signaling Technology, Inc. (Danvers, MA).

2.3. Production of hybridomas

A five-weeks old Sprague–Dawley rat was purchased from CLEA Japan (Tokyo, Japan). All animal experiments were approved by the Animal Care and Use Committee of Tohoku University (Permit number: 2019NiA-001).

To develop mAbs against mCD39, we intraperitoneally immunized one rat with LN229/mCD39 (1×10^9 cells) plus Imject Alum (Thermo Fisher Scientific Inc.). The procedure included three additional injections every week (1×10^9 cells/rat), which were followed by a final booster intraperitoneal injection (1×10^9 cells/rat), two days before the harvest of spleen cells. Hybridomas were produced using PEG1500 (Roche Diagnostics, Indianapolis, IN) as described previously [39]. Supernatants were subsequently screened using flow cytometry, using CHO/mCD39, CHO-K1, L1210, and J774-1 cells.

2.4. Purification of mAbs

The cultured supernatants of C_{39}Mab-1 and C_{39}Mab-2-producing hybridomas were filtered using Steritop (0.22 μm, Merck KGaA, Darmstadt, Germany). Filtered supernatants were subsequently applied to 1 mL of **Protein G Sepharose 4 Fast Flow** (GE Healthcare, Chicago, IL). The bound antibodies were eluted with an IgG elution buffer (Thermo Fisher Scientific Inc.). Finally, eluates were replacd with the elution buffer concentrated, after which PBS was used to replace with phosphate-buffer saline (PBS), using Amicon Ultra (Merck KGaA).

2.5. Flow cytometric analyses

CHO/mCD39 and CHO-K1 were harvested after a brief exposure to 0.25% trypsin and 1 mM ethylenediaminetetraacetic acid (EDTA, Nacalai Tesque, Inc.). Cells were subsequently washed with 0.1% bovine serum albumin (BSA) in PBS and treated with 0.001, 0.01, 0.1, and 1 μg/mL primary mAbs for 30 min at 4°C. Then, cells were treated with anti-rat IgG conjugated with Alexa Fluor 488 or anti-mouse IgG conjugated with Alexa Fluor 488 (1:2000). The fluorescence data were collected using the SA3800 Cell Analyzer (Sony Corp.).

2.6. Determination of dissociation constant (K_D) through flow cytometry

CHO/mCD39 and L1210 were suspended in 100 μL serially-diluted C_{39}Mab-1 and C_{39}Mab-2 for 30 min at 4°C. Then, cells were treated with 50 μL Alexa Fluor 488-conjugated anti-rat IgG (1:200). Then, fluorescence data were collected, using the SA3800 Cell Analyzer. The K_D was subsequently calculated by fitting saturation binding curves to the built-in; one-site binding models in GraphPad PRISM 8 (GraphPad Software, Inc., La Jolla, CA).

2.7. Western blot analysis

Cell lysates were prepared as described previously, and were boiled in sodium dodecyl sulfate (SDS) sample buffer (Nacalai Tesque, Inc.). Protein lysates (10 μg) were separated on 5%–20% polyacrylamide gels (FUJIFILM Wako Pure Chemical Corporation, Osaka, Japan) and transferred onto polyvinylidene difluoride (PVDF) membranes (Merck KGaA). After blocking with 4% skim milk (Nacalai Tesque, Inc.) in PBS with 0.05% Tween 20, membranes were incubated with 10 μg/mL of C_{39}Mab-1 and C_{39}Mab-2, 1 μg/mL of an anti-isocitrate dehydrogenase 1 (IDH1) (clone RcMab-1) [62,63] or 1 μg/mL of NZ-1 (anti-PA tag mAb). Membranes were then incubated with peroxidase-conjugated anti-rat im-

 doi:10.20944/preprints202304.0032.v1

munoglobulins (diluted 1:10000; Sigma-Aldrich Corp., St. Louis, MO, USA). Finally, protein bands were detected with ImmunoStar LD (FUJIFILM Wako Pure Chemical Corporation) using a Sayaca-Imager (DRC Co. Ltd., Tokyo, Japan).

3. Results

3.1. Development of anti-mCD39 mAbs by the CBIS method

To develop anti-mCD39 mAbs, one rat was immunized with LN229/mCD39 cells. (Fig. 1A). The spleen was excised, and the splenocytes were fused with myeloma P3U1 cells (Fig. 1B). Then, positive wells were screened by the selection of mCD39-expressing cell-reactive and CHO-K1-non-reactive supernatants, using flow cytometry (Fig. 1C). After the limiting dilution and several additional screenings, anti-mCD39 mAbs, such as C$_{39}$Mab-1 (rat IgG$_{2a}$, kappa) and C$_{39}$Mab-2 (rat IgG$_{2a}$, lambda) were finally established (Fig. 1D).

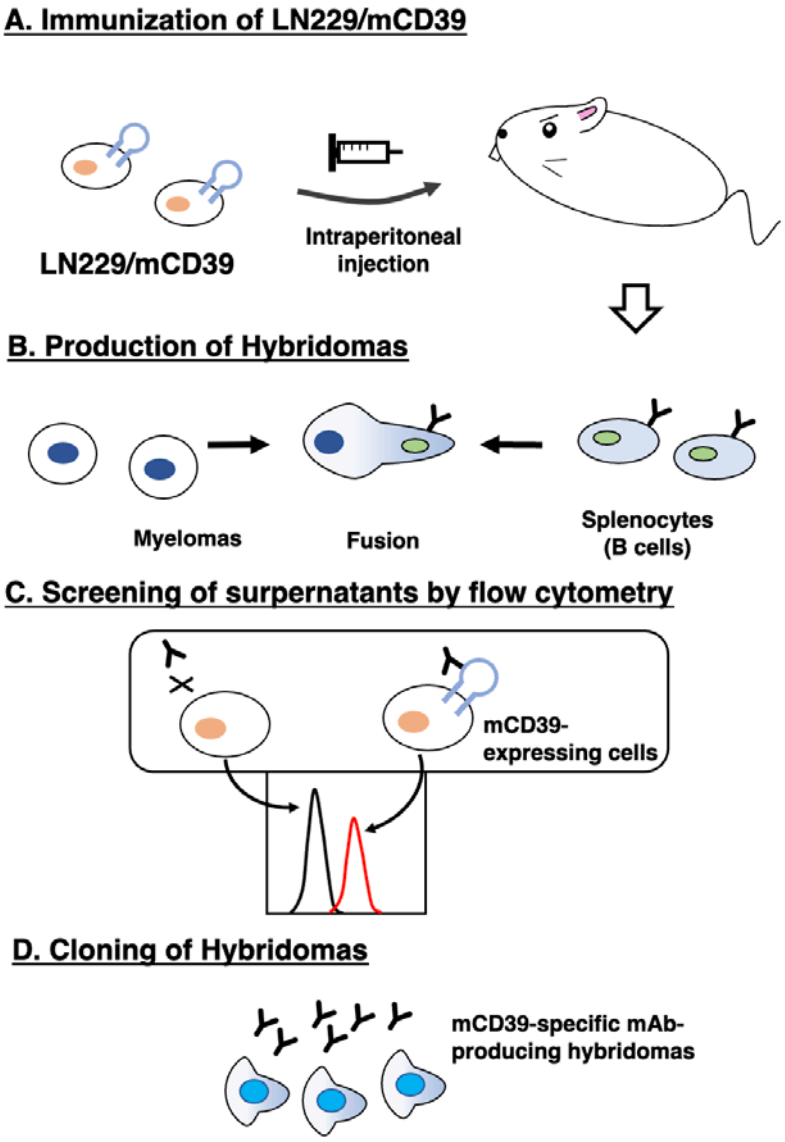

Figure 1. A schematic illustration showing the production of anti-mCD39 mAbs. (A) CD39 is anchored to the membrane by two transmembrane domains at the two ends of the molecule. LN229/mCD39 cells was immunized into an SD rat, using an intraperitoneal injection. (B) Spleen cells were then fused with P3U1 cells. (C) The culture supernatants were screened through flow cytometry to select anti-mCD39 mAb-producing hybridomas. (D) After limiting dilution, anti-mCD39 mAbs were finally established.

 doi:10.20944/preprints202304.0032.v1

3.2. Flow cytometric analyses

We performed flow cytometry using three anti-mCD39 mAbs: C39Mab-1, C39Mab-2, and 5F2 against CHO/mCD39, L1210, and J774-1 cell lines. Both C39Mab-1 and C39Mab-2 recognized CHO/mCD39 cells dose-dependently at 1, 0.1, 0.01, and 0.001 μg/ml. In contrast, 5F2 needed more than 0.01 μg/ml for the detection of CHO/mCD39 (Fig. 2A). Parental CHO-K1 cells were not recognized even at 1 μg/ml of all mAbs (Fig. 2B).

Furthermore, we investigated the reactivity of C39Mab-1 and C39Mab-2 against endogenously mCD39-expressed cell lines, such as L1210 (mouse lymphocytic leukemia) and J774-1 (mouse macrophage-like). C39Mab-1 and C39Mab-2 reacted with L1210 and J774-1 cells at more than 0.1 μg/ml (Fig. 3A and B). In contrast, 5F2 could not clearly reacted with L1210 and J774-1 cells at 1 μg/ml. 5F2 could detect them at 10 μg/ml (data not shown). These results suggested that C39Mab-1 and C39Mab-2 specifically recognizes mCD39, and is also useful for detecting endogenous mCD39 by flow cytometry.

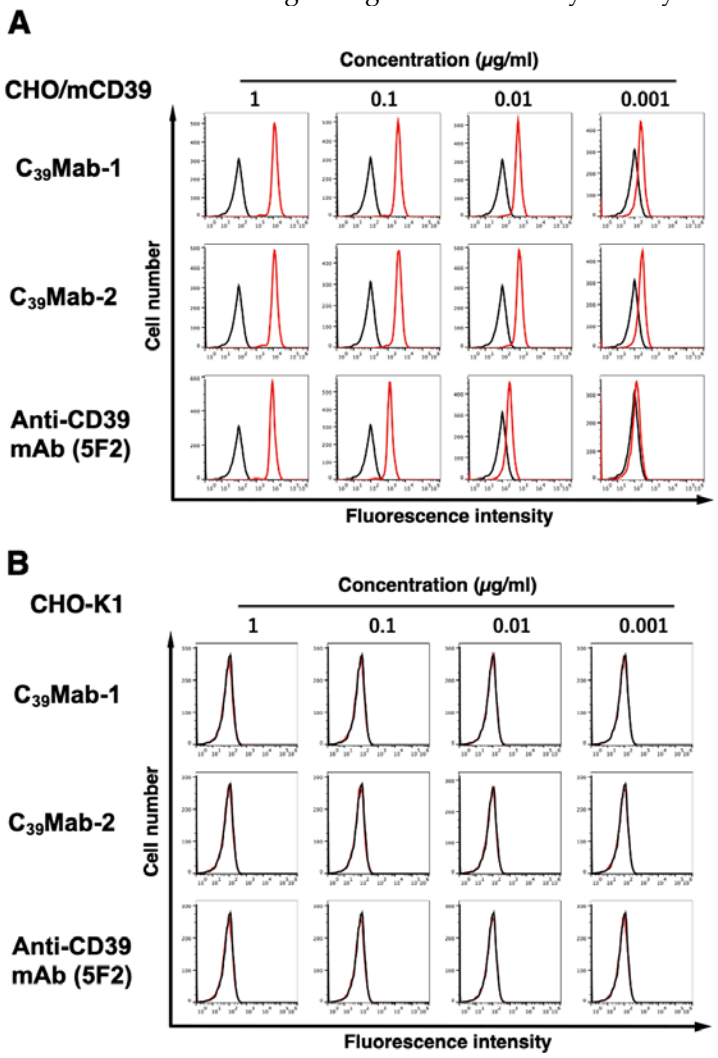

Figure 2. Flow cytometry to mCD39-overexpressing cells using anti-mCD39 mAbs. CHO/mCD39 (A) and CHO-K1 (B) cells were treated with 0.001–1 μg/mL of C39Mab-1, C39Mab-2 and 5F2, followed by treatment with anti-rat IgG conjugated with Alexa Fluor 488 (for C39Mab-1 and C39Mab-2) or anti-mouse IgG conjugated with Alexa Fluor 488 (for 5F2). Black line represents the negative control.

Preprints (www.preprints.org) | NOT PEER-REVIEWED | Posted: 4 April 2023 doi:10.20944/preprints202304.0032.v1

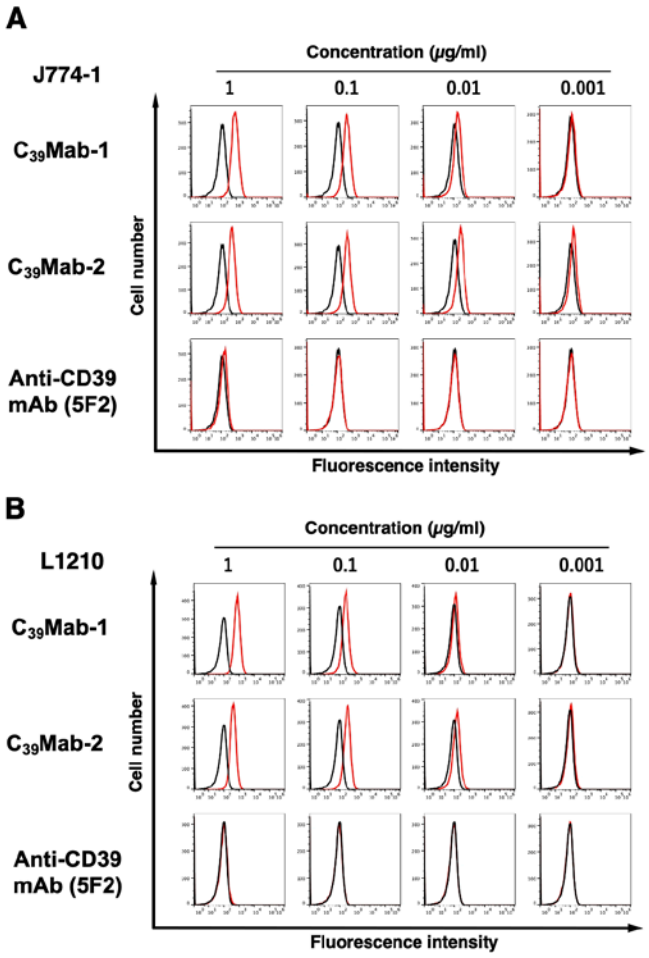

Figure 3. Flow cytometry to endogenously mCD39-expressing cells using anti- mCD39 mAbs. J-774-1 (A) and L1210 (B) cells were treated with 0.001–1 μg/mL of C39Mab-1, C39Mab-2, and 5F2, followed by treatment with anti-rat IgG conjugated with Alexa Fluor 488 (for C39Mab-1 and C39Mab-2) or anti-mouse IgG conjugated with Alexa Fluor 488 (for 5F2). Black line represents the negative control.

3.3. Kinetic analyses of C39Mab-1 and C39Mab-2 against mCD39-expressing cells using flow cytometry

To determine the K_D of C39Mab-1 and C39Mab-2 with mCD39-expressing cells, we conducted kinetic analysis by flow cytometry using CHO/mCD39 and L1210 cells. The K_D values of C39Mab-1 and C39Mab-2 for CHO/mCD39 were determined as 7.3×10^{-9} M and 5.5×10^{-9} M, respectively (Fig. 4A and B). Furthermore, The K_D values of C39Mab-1 and C39Mab-2 for L1210 were determined as 3.3×10^{-9} M and 3.6×10^{-10} M, respectively (Fig. 4C and D). These results indicate that C39Mab-1 and C39Mab-2 possess the high affinity for both CHO/mCD39 and L1210 cells.

Preprints (www.preprints.org) | NOT PEER-REVIEWED | Posted: 4 April 2023 doi:10.20944/preprints202304.0032.v1

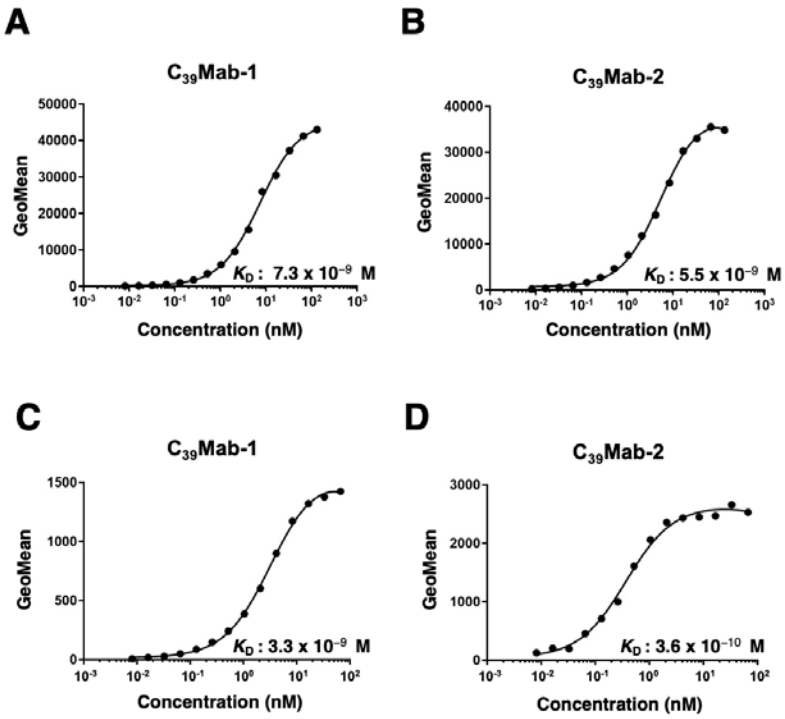

Figure 4. The determination of the binding affinity of Cx6Mab-1. CHO/mCD39 (A and B) and L1210 (C and D) cells were suspended in 100 μL serially diluted C39Mab-1 and C39Mab-2 at indicated concentrations. Then, cells were treated with Alexa Fluor 488-conjugated anti-rat IgG. Fluorescence data were subsequently collected using the SA3800 Cell Analyzer, following the calculation of the dissociation constant (*K*D) by GraphPad PRISM 8.

3.4. Western blot analyses

Western blotting was performed to further assess the specificity of C39Mab-1 and C39Mab-2. Cell lysates of CHO-K1 and CHO/mCD39 were probed. As shown in Fig. 5A, C39Mab-1 detected mCD39 as a ~100-kDa band. However, C39Mab-2 did not detect any bands from lysates of CHO-K1 and CHO/mCD39 cells (Fig. 5B). An anti-PA tag mAb (clone NZ-1) recognized the lysates from CHO/ mCD39 (~100 kDa, mainly) (Fig. 5C). These results indicated that C39Mab-1 can detect mCD39 specifically by western blot analysis.

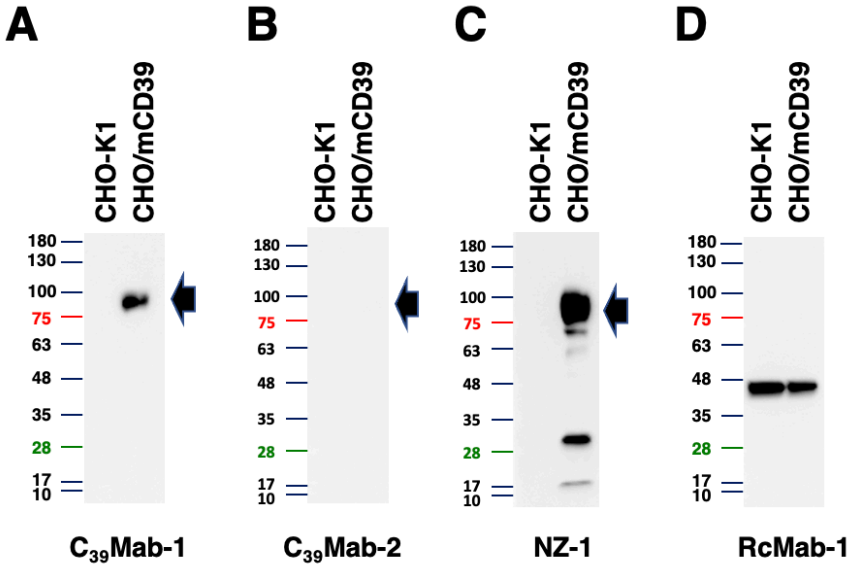

 doi:10.20944/preprints202304.0032.v1

Figure 5. Western blotting using C39Mab-1 and C39Mab-2. Cell lysates of CHO-K1 and CHO/mCD39 were electrophoresed and transferred onto polyvinylidene fluoride (PVDF) membranes. The membranes were incubated with 10 μg/mL of C39Mab-1 (A), 10 μg/mL of C39Mab-2 (B), 1 μg/mL of NZ-1 (an anti-PA tag mAb) (C), or 1 μg/mL of RcMab-1 (an anti-IDH mAb) (D). Membranes were subsequently incubated with peroxidase-conjugated anti-rat immunoglobulins. Arrows indicate the predicted size of mCD39 (~100 kDa).

4. Discussion

In this study, we developed novel anti-mCD39 mAbs (C39Mab-1 and C39Mab-2) using the CBIS method, and investigated the usefulness for flow cytometry and western blotting for detecting mCD39. C39Mab-1 is available for both flow cytometry (Fig. 2 and 3) and western blot analysis (Fig. 5). C39Mab-2 is available only for flow cytometry (Fig. 2 and 3), but exhibited the higher affinity to mCD39 expressing cells than C39Mab-1 (Fig. 4). To assess the difference of the properties, the identification of the epitope is essential. We have developed the REMAP method [64-67] to determine the epitope of mAbs. The conformational epitopes of anti-EGFR mAbs (EMab-51 and EMab-134) [65,67] and anti-CD44 mAbs (C44Mab-5 and C44Mab-46) [64,66] could be determined using the REMAP method. Therefore, further studies are required to determine the epitope of C39Mab-1 and C39Mab-2.

In the TME, extracellular levels of ATP can reach to 100 to 500 μM compared to nanomolar order in normal tissues [9]. CD39 can rapidly hydrolyzed and convert to adenosine in cooperation with CD73. In this TME, an enzymatic inhibitor of CD39 is the rational mechanism to inhibit the production of immunosuppressive adenosine. The clinically tested anti-CD39 mAb, TTX-030 (human IgG_4), had a subnanomolar EC_{50} for human CD39-overexpressed CHO cells in flow cytometry-based assay like Fig. 3. Furthermore, TTX-030 allosterically inhibited the enzymatic activity of CD39 in recombinant human CD39 extracellular domain and membrane-bound cellular CD39 [68]. We will investigate the effect of C39Mab-1 and C39Mab-2 on the enzymatic activity of mCD39 in the future study.

Recently, Zhang *et al.* [69] demonstrated the application of an anti-mCD39 mAb for tumor therapy by the depletion of immunosuppressive cells through enhanced Fcγ receptor–mediated antibody-dependent cellular cytotoxicity (ADCC). They found that mCD39 expression on tumor-infiltrating immune and vascular endothelial cells is markedly higher than in normal tissues. They used a non-neutralizing anti-mCD39 mAb (clone 5F2, mouse IgG_1), and screened an isotype-switched hybridoma subline of the IgG_{2c} isotype which has more potent ADCC activities. To enhance the effector functions, the fucosyltransferase 8 (Fut8) gene was deleted in the 5F2 hybridomas using CRISPR to produce the afucosylated antibody. They showed that the afucosylated anti-mCD39 IgG_{2c} exerted the potent antitumor effect against mouse melanoma and colorectal tumor models through the depletion of regulatory/exhausted T cells, tumor-associated macrophages and tumor vasculature with high mCD39 expression.

We previously produced recombinant antibodies, which are converted into mouse IgG_{2a} subclass from mouse IgG_1. Furthermore, we produced afucosylated IgG_{2a} mAbs using Fut8-deficient CHO-K1 cells to potentiate the ADCC activity. The afucosylated mAbs showed potent antitumor activity in mouse xenograft models [70-77]. Therefore, a class-switched and afucosylated version of C39Mab-1 or C39Mab-2 could be used to evaluate the antitumor activity *in vivo*.

Author Contributions: HS, Y.Kudo, MT, NG, KI, TO, TT, TA, TN, and MY performed the experiments. MKK and Y.Kato designed the experiments. HS, and Y.Kato analyzed the data. HS, and Y.Kato wrote the manuscript. All authors read and approved the final manuscript and agreed to be accountable for all aspects of the research in ensuring that the accuracy or integrity of any part of the work is appropriately investigated and resolved.

Funding: This research was supported in part by Japan Agency for Medical Research and Development (AMED) under Grant Numbers: JP22ama121008 (to Y.K.), JP22am0401013 (to Y.K.), JP22bm1004001 (to Y.K.), JP22ck0106730 (to Y.K.), and JP21am0101078 (to Y.K.), and by the Japan

Society for the Promotion of Science (JSPS) Grants-in-Aid for Scientific Research (KAKENHI) grant nos. 21K20789 (to T.T.), 22K06995 (to H.S.), 21K07168 (to M.K.K.), and 22K07224 (to Y.K.).

Institutional Review Board Statement: The animal study protocol was approved by the Animal Care and Use Committee of Tohoku University (Permit number: 2019NiA-001) for studies involving animals.

Data Availability Statement: All related data and methods are presented in this paper. Additional inquiries should be addressed to the corresponding authors.

Conflicts of Interest: The authors declare no conflict of interest involving this article.

References

1. Guo, S.; Han, F.; Zhu, W. CD39 - A bright target for cancer immunotherapy. *Biomed Pharmacother* **2022**, *151*, 113066, doi:10.1016/j.biopha.2022.113066.
2. Grygorczyk, R.; Boudreault, F.; Ponomarchuk, O.; Tan, J.J.; Furuya, K.; Goldgewicht, J.; Kenfack, F.D.; Yu, F. Lytic Release of Cellular ATP: Physiological Relevance and Therapeutic Applications. *Life (Basel)* **2021**, *11*, doi:10.3390/life11070700.
3. Moesta, A.K.; Li, X.Y.; Smyth, M.J. Targeting CD39 in cancer. *Nat Rev Immunol* **2020**, *20*, 739-755, doi:10.1038/s41577-020-0376-4.
4. Churov, A.; Zhulai, G. Targeting adenosine and regulatory T cells in cancer immunotherapy. *Hum Immunol* **2021**, *82*, 270-278, doi:10.1016/j.humimm.2020.12.005.
5. Vijayan, D.; Young, A.; Teng, M.W.L.; Smyth, M.J. Targeting immunosuppressive adenosine in cancer. *Nat Rev Cancer* **2017**, *17*, 709-724, doi:10.1038/nrc.2017.86.
6. Sun, C.; Wang, B.; Hao, S. Adenosine-A2A Receptor Pathway in Cancer Immunotherapy. *Front Immunol* **2022**, *13*, 837230, doi:10.3389/fimmu.2022.837230.
7. Ohta, A.; Sitkovsky, M. Role of G-protein-coupled adenosine receptors in downregulation of inflammation and protection from tissue damage. *Nature* **2001**, *414*, 916-920, doi:10.1038/414916a.
8. Ohta, A.; Gorelik, E.; Prasad, S.J.; Ronchese, F.; Lukashev, D.; Wong, M.K.; Huang, X.; Caldwell, S.; Liu, K.; Smith, P.; et al. A2A adenosine receptor protects tumors from antitumor T cells. *Proc Natl Acad Sci U S A* **2006**, *103*, 13132-13137, doi:10.1073/pnas.0605251103.
9. Di Virgilio, F.; Sarti, A.C.; Falzoni, S.; De Marchi, E.; Adinolfi, E. Extracellular ATP and P2 purinergic signalling in the tumour microenvironment. *Nat Rev Cancer* **2018**, *18*, 601-618, doi:10.1038/s41568-018-0037-0.
10. Li, X.Y.; Moesta, A.K.; Xiao, C.; Nakamura, K.; Casey, M.; Zhang, H.; Madore, J.; Lepletier, A.; Aguilera, A.R.; Sundarrajan, A.; et al. Targeting CD39 in Cancer Reveals an Extracellular ATP- and Inflammasome-Driven Tumor Immunity. *Cancer Discov* **2019**, *9*, 1754-1773, doi:10.1158/2159-8290.Cd-19-0541.
11. Perrot, I.; Michaud, H.A.; Giraudon-Paoli, M.; Augier, S.; Docquier, A.; Gros, L.; Courtois, R.; Déjou, C.; Jecko, D.; Becquart, O.; et al. Blocking Antibodies Targeting the CD39/CD73 Immunosuppressive Pathway Unleash Immune Responses in Combination Cancer Therapies. *Cell Rep* **2019**, *27*, 2411-2425.e2419, doi:10.1016/j.celrep.2019.04.091.
12. Yamada, S.; Kaneko, M.K.; Sayama, Y.; Asano, T.; Sano, M.; Yanaka, M.; Nakamura, T.; Okamoto, S.; Handa, S.; Komatsu, Y.; et al. Development of Novel Mouse Monoclonal Antibodies Against Human CD19. *Monoclon Antib Immunodiagn Immunother* **2020**, *39*, 45-50, doi:10.1089/mab.2020.0003.
13. Furusawa, Y.; Kaneko, M.K.; Kato, Y. Establishment of C(20)Mab-11, a novel anti-CD20 monoclonal antibody, for the detection of B cells. *Oncol Lett* **2020**, *20*, 1961-1967, doi:10.3892/ol.2020.11753.
14. Furusawa, Y.; Kaneko, M.K.; Kato, Y. Establishment of an Anti-CD20 Monoclonal Antibody (C(20)Mab-60) for Immunohistochemical Analyses. *Monoclon Antib Immunodiagn Immunother* **2020**, *39*, 112-116, doi:10.1089/mab.2020.0015.
15. Itai, S.; Fujii, Y.; Nakamura, T.; Chang, Y.W.; Yanaka, M.; Saidoh, N.; Handa, S.; Suzuki, H.; Harada, H.; Yamada, S.; et al. Establishment of CMab-43, a Sensitive and Specific Anti-CD133 Monoclonal Antibody, for Immunohistochemistry. *Monoclon Antib Immunodiagn Immunother* **2017**, *36*, 231-235, doi:10.1089/mab.2017.0031.
16. Li, G.; Suzuki, H.; Asano, T.; Tanaka, T.; Suzuki, H.; Kaneko, M.K.; Kato, Y. Development of a Novel Anti-EpCAM Monoclonal Antibody for Various Applications. *Antibodies (Basel)* **2022**, *11*, doi:10.3390/antib11020041.
17. Kaneko, M.K.; Ohishi, T.; Takei, J.; Sano, M.; Nakamura, T.; Hosono, H.; Yanaka, M.; Asano, T.; Sayama, Y.; Harada, H.; et al. Anti-EpCAM monoclonal antibody exerts antitumor activity against oral squamous cell carcinomas. *Oncol Rep* **2020**, *44*, 2517-2526, doi:10.3892/or.2020.7808.
18. Itai, S.; Fujii, Y.; Kaneko, M.K.; Yamada, S.; Nakamura, T.; Yanaka, M.; Saidoh, N.; Chang, Y.W.; Handa, S.; Takahashi, M.; et al. H(2)Mab-77 is a Sensitive and Specific Anti-HER2 Monoclonal Antibody Against Breast Cancer. *Monoclon Antib Immunodiagn Immunother* **2017**, *36*, 143-148, doi:10.1089/mab.2017.0026.
19. Asano, T.; Ohishi, T.; Takei, J.; Nakamura, T.; Nanamiya, R.; Hosono, H.; Tanaka, T.; Sano, M.; Harada, H.; Kawada, M.; et al. Anti-HER3 monoclonal antibody exerts antitumor activity in a mouse model of colorectal adenocarcinoma. *Oncol Rep* **2021**, *46*, doi:10.3892/or.2021.8124.
20. Asano, T.; Nanamiya, R.; Tanaka, T.; Kaneko, M.K.; Kato, Y. Development of Antihuman Killer Cell Lectin-Like Receptor Subfamily G Member 1 Monoclonal Antibodies for Flow Cytometry. *Monoclon Antib Immunodiagn Immunother* **2021**, *40*, 76-80, doi:10.1089/mab.2021.0008.

21. Takei, J.; Asano, T.; Nanamiya, R.; Nakamura, T.; Yanaka, M.; Hosono, H.; Tanaka, T.; Sano, M.; Kaneko, M.K.; Harada, H.; et al. Development of Anti-human T Cell Immunoreceptor with Ig and ITIM Domains (TIGIT) Monoclonal Antibodies for Flow Cytometry. *Monoclon Antib Immunodiagn Immunother* **2021**, *40*, 71-75, doi:10.1089/mab.2021.0006.
22. Sayama, Y.; Kaneko, M.K.; Takei, J.; Hosono, H.; Sano, M.; Asano, T.; Kato, Y. Establishment of a novel anti-TROP2 monoclonal antibody TrMab-29 for immunohistochemical analysis. *Biochem Biophys Rep* **2021**, *25*, 100902, doi:10.1016/j.bbrep.2020.100902.
23. Tanaka, T.; Ohishi, T.; Asano, T.; Takei, J.; Nanamiya, R.; Hosono, H.; Sano, M.; Harada, H.; Kawada, M.; Kaneko, M.K.; et al. An anti-TROP2 monoclonal antibody TrMab-6 exerts antitumor activity in breast cancer mouse xenograft models. *Oncol Rep* **2021**, *46*, doi:10.3892/or.2021.8083.
24. Yamada, S.; Itai, S.; Nakamura, T.; Yanaka, M.; Chang, Y.W.; Suzuki, H.; Kaneko, M.K.; Kato, Y. Monoclonal Antibody L(1)Mab-13 Detected Human PD-L1 in Lung Cancers. *Monoclon Antib Immunodiagn Immunother* **2018**, *37*, 110-115, doi:10.1089/mab.2018.0004.
25. Yamada, S.; Itai, S.; Nakamura, T.; Yanaka, M.; Saidoh, N.; Chang, Y.W.; Handa, S.; Harada, H.; Kagawa, Y.; Ichii, O.; et al. PMab-52: Specific and Sensitive Monoclonal Antibody Against Cat Podoplanin for Immunohistochemistry. *Monoclon Antib Immunodiagn Immunother* **2017**, *36*, 224-230, doi:10.1089/mab.2017.0027.
26. Furusawa, Y.; Kaneko, M.K.; Nakamura, T.; Itai, S.; Fukui, M.; Harada, H.; Yamada, S.; Kato, Y. Establishment of a Monoclonal Antibody PMab-231 for Tiger Podoplanin. *Monoclon Antib Immunodiagn Immunother* **2019**, *38*, 89-95, doi:10.1089/mab.2019.0003.
27. Furusawa, Y.; Takei, J.; Sayama, Y.; Yamada, S.; Kaneko, M.K.; Kato, Y. Development of an anti-bear podoplanin monoclonal antibody PMab-247 for immunohistochemical analysis. *Biochem Biophys Rep* **2019**, *18*, 100644, doi:10.1016/j.bbrep.2019.100644.
28. Furusawa, Y.; Yamada, S.; Itai, S.; Nakamura, T.; Takei, J.; Sano, M.; Harada, H.; Fukui, M.; Kaneko, M.K.; Kato, Y. Establishment of a monoclonal antibody PMab-233 for immunohistochemical analysis against Tasmanian devil podoplanin. *Biochem Biophys Rep* **2019**, *18*, 100631, doi:10.1016/j.bbrep.2019.100631.
29. Goto, N.; Suzuki, H.; Tanaka, T.; Asano, T.; Kaneko, M.K.; Kato, Y. Development of a Monoclonal Antibody PMab-292 Against Ferret Podoplanin. *Monoclon Antib Immunodiagn Immunother* **2022**, 41, 101-109, doi: 10.1089/mab.2021.0067.
30. Furusawa, Y.; Yamada, S.; Itai, S.; Sano, M.; Nakamura, T.; Yanaka, M.; Handa, S.; Mizuno, T.; Maeda, K.; Fukui, M.; et al. Establishment of Monoclonal Antibody PMab-202 Against Horse Podoplanin. *Monoclon. Antib. Immunodiagn. Immunother.* **2018**, *37*, 233-237, doi:10.1089/mab.2018.0030.
31. Kato, Y.; Yamada, S.; Furusawa, Y.; Itai, S.; Nakamura, T.; Yanaka, M.; Sano, M.; Harada, H.; Fukui, M.; Kaneko, M.K. PMab-213: a monoclonal antibody for immunohistochemical analysis against pig podoplanin. *Monoclon. Antib. Immunodiagn. Immunother.* **2019**, *38*, 18-24.
32. Furusawa, Y.; Yamada, S.; Nakamura, T.; Sano, M.; Sayama, Y.; Itai, S.; Takei, J.; Harada, H.; Fukui, M.; Kaneko, M.K.; et al. PMab-235: A monoclonal antibody for immunohistochemical analysis against goat podoplanin. *Heliyon* **2019**, *5*, e02063, doi:10.1016/j.heliyon.2019.e02063.
33. Kato, Y.; Furusawa, Y.; Yamada, S.; Itai, S.; Takei, J.; Sano, M.; Kaneko, M.K. Establishment of a monoclonal antibody PMab-225 against alpaca podoplanin for immunohistochemical analyses. *Biochem Biophys Rep* **2019**, *18*, 100633, doi:10.1016/j.bbrep.2019.100633.
34. Kato, Y.; Furusawa, Y.; Itai, S.; Takei, J.; Nakamura, T.; Sano, M.; Harada, H.; Yamada, S.; Kaneko, M.K. Establishment of an Anticetacean Podoplanin Monoclonal Antibody PMab-237 for Immunohistochemical Analysis. *Monoclon. Antib. Immunodiagn. Immunother.* **2019**, *38*, 108–113.
35. Kato, Y.; Furusawa, Y.; Sano, M.; Takei, J.; Nakamura, T.; Yanaka, M.; Okamoto, S.; Handa, S.; Komatsu, Y.; Asano, T.; et al. Development of an Anti-Sheep Podoplanin Monoclonal Antibody PMab-256 for Immunohistochemical Analysis of Lymphatic Endothelial Cells. *Monoclon Antib Immunodiagn Immunother* **2020**, *39*, 82-90, doi:10.1089/mab.2020.0005.
36. Tanaka, T.; Asano, T.; Sano, M.; Takei, J.; Hosono, H.; Nanamiya, R.; Nakamura, T.; Yanaka, M.; Harada, H.; Fukui, M.; et al. Development of Monoclonal Antibody PMab-269 Against California Sea Lion Podoplanin. *Monoclon Antib Immunodiagn Immunother* **2021**, *40*, 124-133, doi:10.1089/mab.2021.0011.
37. Ejima, R.; Suzuki, H.; Tanaka, T.; Asano, T.; Kaneko, M.K.; Kato, Y. Development of a Novel Anti-CD44 Variant 6 Monoclonal Antibody C(44)Mab-9 for Multiple Applications against Colorectal Carcinomas. *Int J Mol Sci* **2023**, *24*, doi:10.3390/ijms24044007.
38. Yamada, S.; Itai, S.; Nakamura, T.; Yanaka, M.; Kaneko, M.K.; Kato, Y. Detection of high CD44 expression in oral cancers using the novel monoclonal antibody, C(44)Mab-5. *Biochem Biophys Rep* **2018**, *14*, 64-68, doi:10.1016/j.bbrep.2018.03.007.
39. Asano, T.; Nanamiya, R.; Takei, J.; Nakamura, T.; Yanaka, M.; Hosono, H.; Tanaka, T.; Sano, M.; Kaneko, M.K.; Kato, Y. Development of Anti-Mouse CC Chemokine Receptor 3 Monoclonal Antibodies for Flow Cytometry. *Monoclon Antib Immunodiagn Immunother* **2021**, *40*, 107-112, doi:10.1089/mab.2021.0009.
40. Tanaka, T.; Nanamiya, R.; Takei, J.; Nakamura, T.; Yanaka, M.; Hosono, H.; Sano, M.; Asano, T.; Kaneko, M.K.; Kato, Y. Development of Anti-Mouse CC Chemokine Receptor 8 Monoclonal Antibodies for Flow Cytometry. *Monoclon Antib Immunodiagn Immunother* **2021**, *40*, 65-70, doi:10.1089/mab.2021.0005.
41. Nanamiya, R.; Takei, J.; Asano, T.; Tanaka, T.; Sano, M.; Nakamura, T.; Yanaka, M.; Hosono, H.; Kaneko, M.K.; Kato, Y. Development of Anti-Human CC Chemokine Receptor 9 Monoclonal Antibodies for Flow Cytometry. *Monoclon Antib Immunodiagn Immunother* **2021**, *40*, 101-106, doi:10.1089/mab.2021.0007.
42. Tamura, R.; Oi, R.; Akashi, S.; Kaneko, M.K.; Kato, Y.; Nogi, T. Application of the NZ-1 Fab as a crystallization chaperone for PA tag-inserted target proteins. *Protein Sci* **2019**, *28*, 823-836, doi:10.1002/pro.3580.

43. Fujii, Y.; Matsunaga, Y.; Arimori, T.; Kitago, Y.; Ogasawara, S.; Kaneko, M.K.; Kato, Y.; Takagi, J. Tailored placement of a turn-forming PA tag into the structured domain of a protein to probe its conformational state. *J Cell Sci* **2016**, *129*, 1512-1522, doi:10.1242/jcs.176685.
44. Fujii, Y.; Kaneko, M.; Neyazaki, M.; Nogi, T.; Kato, Y.; Takagi, J. PA tag: a versatile protein tagging system using a super high affinity antibody against a dodecapeptide derived from human podoplanin. *Protein Expr Purif* **2014**, *95*, 240-247, doi:10.1016/j.pep.2014.01.009.
45. Miura, K.; Yoshida, H.; Nosaki, S.; Kaneko, M.K.; Kato, Y. RAP Tag and PMab-2 Antibody: A Tagging System for Detecting and Purifying Proteins in Plant Cells. *Front Plant Sci* **2020**, *11*, 510444, doi:10.3389/fpls.2020.510444.
46. Fujii, Y.; Kaneko, M.K.; Ogasawara, S.; Yamada, S.; Yanaka, M.; Nakamura, T.; Saidoh, N.; Yoshida, K.; Honma, R.; Kato, Y. Development of RAP Tag, a Novel Tagging System for Protein Detection and Purification. *Monoclon Antib Immunodiagn Immunother* **2017**, *36*, 68-71, doi:10.1089/mab.2016.0052.
47. Fujii, Y.; Kaneko, M.K.; Kato, Y. MAP Tag: A Novel Tagging System for Protein Purification and Detection. *Monoclon Antib Immunodiagn Immunother* **2016**, *35*, 293-299, doi:10.1089/mab.2016.0039.
48. Wakasa, A.; Kaneko, M.K.; Kato, Y.; Takagi, J.; Arimori, T. Site-specific epitope insertion into recombinant proteins using the MAP tag system. *J Biochem* **2020**, *168*, 375-384, doi:10.1093/jb/mvaa054.
49. Kato, Y.; Kaneko, M.K.; Kuno, A.; Uchiyama, N.; Amano, K.; Chiba, Y.; Hasegawa, Y.; Hirabayashi, J.; Narimatsu, H.; Mishima, K.; et al. Inhibition of tumor cell-induced platelet aggregation using a novel anti-podoplanin antibody reacting with its platelet-aggregation-stimulating domain. *Biochem Biophys Res Commun* **2006**, *349*, 1301-1307, doi:10.1016/j.bbrc.2006.08.171.
50. Chalise, L.; Kato, A.; Ohno, M.; Maeda, S.; Yamamichi, A.; Kuramitsu, S.; Shiina, S.; Takahashi, H.; Ozone, S.; Yamaguchi, J.; et al. Efficacy of cancer-specific anti-podoplanin CAR-T cells and oncolytic herpes virus G47Delta combination therapy against glioblastoma. *Mol Ther Oncolytics* **2022**, *26*, 265-274, doi:10.1016/j.omto.2022.07.006.
51. Ishikawa, A.; Waseda, M.; Ishii, T.; Kaneko, M.K.; Kato, Y.; Kaneko, S. Improved anti-solid tumor response by humanized anti-podoplanin chimeric antigen receptor transduced human cytotoxic T cells in an animal model. *Genes Cells* **2022**, *27*, 549-558, doi:10.1111/gtc.12972.
52. Tamura-Sakaguchi, R.; Aruga, R.; Hirose, M.; Ekimoto, T.; Miyake, T.; Hizukuri, Y.; Oi, R.; Kaneko, M.K.; Kato, Y.; Akiyama, Y.; et al. Moving toward generalizable NZ-1 labeling for 3D structure determination with optimized epitope-tag insertion. *Acta Crystallogr D Struct Biol* **2021**, *77*, 645-662, doi:10.1107/S2059798321002527.
53. Kaneko, M.K.; Ohishi, T.; Nakamura, T.; Inoue, H.; Takei, J.; Sano, M.; Asano, T.; Sayama, Y.; Hosono, H.; Suzuki, H.; et al. Development of Core-Fucose-Deficient Humanized and Chimeric Anti-Human Podoplanin Antibodies. *Monoclon Antib Immunodiagn Immunother* **2020**, *39*, 167-174, doi:10.1089/mab.2020.0019.
54. Abe, S.; Kaneko, M.K.; Tsuchihashi, Y.; Izumi, T.; Ogasawara, S.; Okada, N.; Sato, C.; Tobiume, M.; Otsuka, K.; Miyamoto, L.; et al. Antitumor effect of novel anti-podoplanin antibody NZ-12 against malignant pleural mesothelioma in an orthotopic xenograft model. *Cancer Sci* **2016**, *107*, 1198-1205, doi:10.1111/cas.12985.
55. Kaneko, M.K.; Abe, S.; Ogasawara, S.; Fujii, Y.; Yamada, S.; Murata, T.; Uchida, H.; Tahara, H.; Nishioka, Y.; Kato, Y. Chimeric Anti-Human Podoplanin Antibody NZ-12 of Lambda Light Chain Exerts Higher Antibody-Dependent Cellular Cytotoxicity and Complement-Dependent Cytotoxicity Compared with NZ-8 of Kappa Light Chain. *Monoclon Antib Immunodiagn Immunother* **2017**, *36*, 25-29, doi:10.1089/mab.2016.0047.
56. Ito, A.; Ohta, M.; Kato, Y.; Inada, S.; Kato, T.; Nakata, S.; Yatabe, Y.; Goto, M.; Kaneda, N.; Kurita, K.; et al. A Real-Time Near-Infrared Fluorescence Imaging Method for the Detection of Oral Cancers in Mice Using an Indocyanine Green-Labeled Podoplanin Antibody. *Technol Cancer Res Treat* **2018**, *17*, 1533033818767936, doi:10.1177/1533033818767936.
57. Shiina, S.; Ohno, M.; Ohka, F.; Kuramitsu, S.; Yamamichi, A.; Kato, A.; Motomura, K.; Tanahashi, K.; Yamamoto, T.; Watanabe, R.; et al. CAR T Cells Targeting Podoplanin Reduce Orthotopic Glioblastomas in Mouse Brains. *Cancer Immunol Res* **2016**, *4*, 259-268, doi:10.1158/2326-6066.CIR-15-0060.
58. Kuwata, T.; Yoneda, K.; Mori, M.; Kanayama, M.; Kuroda, K.; Kaneko, M.K.; Kato, Y.; Tanaka, F. Detection of Circulating Tumor Cells (CTCs) in Malignant Pleural Mesothelioma (MPM) with the "Universal" CTC-Chip and An Anti-Podoplanin Antibody NZ-1.2. *Cells* **2020**, *9*, doi:10.3390/cells9040888.
59. Nishinaga, Y.; Sato, K.; Yasui, H.; Taki, S.; Takahashi, K.; Shimizu, M.; Endo, R.; Koike, C.; Kuramoto, N.; Nakamura, S.; et al. Targeted Phototherapy for Malignant Pleural Mesothelioma: Near-Infrared Photoimmunotherapy Targeting Podoplanin. *Cells* **2020**, *9*, doi:10.3390/cells9041019.
60. Kato, Y.; Kaneko, M.K.; Kunita, A.; Ito, H.; Kameyama, A.; Ogasawara, S.; Matsuura, N.; Hasegawa, Y.; Suzuki-Inoue, K.; Inoue, O.; et al. Molecular analysis of the pathophysiological binding of the platelet aggregation-inducing factor podoplanin to the C-type lectin-like receptor CLEC-2. *Cancer Sci* **2008**, *99*, 54-61, doi:10.1111/j.1349-7006.2007.00634.x.
61. Kato, Y.; Vaidyanathan, G.; Kaneko, M.K.; Mishima, K.; Srivastava, N.; Chandramohan, V.; Pegram, C.; Keir, S.T.; Kuan, C.T.; Bigner, D.D.; et al. Evaluation of anti-podoplanin rat monoclonal antibody NZ-1 for targeting malignant gliomas. *Nucl Med Biol* **2010**, *37*, 785-794, doi:10.1016/j.nucmedbio.2010.03.010.
62. Kato, Y. Specific monoclonal antibodies against IDH1/2 mutations as diagnostic tools for gliomas. *Brain Tumor Pathol* **2015**, *32*, 3-11, doi:10.1007/s10014-014-0202-4.
63. Ikota, H.; Nobusawa, S.; Arai, H.; Kato, Y.; Ishizawa, K.; Hirose, T.; Yokoo, H. Evaluation of IDH1 status in diffusely infiltrating gliomas by immunohistochemistry using anti-mutant and wild type IDH1 antibodies. *Brain Tumor Pathol* **2015**, *32*, 237-244, doi:10.1007/s10014-015-0222-8.

64. Asano, T.; Kaneko, M.K.; Takei, J.; Tateyama, N.; Kato, Y. Epitope Mapping of the Anti-CD44 Monoclonal Antibody (C44Mab-46) Using the REMAP Method. *Monoclon Antib Immunodiagn Immunother* **2021**, *40*, 156-161, doi:10.1089/mab.2021.0012.
65. Sano, M.; Kaneko, M.K.; Aasano, T.; Kato, Y. Epitope Mapping of an Antihuman EGFR Monoclonal Antibody (EMab-134) Using the REMAP Method. *Monoclon Antib Immunodiagn Immunother* **2021**, *40*, 191-195, doi:10.1089/mab.2021.0014.
66. Asano, T.; Kaneko, M.K.; Kato, Y. Development of a Novel Epitope Mapping System: RIEDL Insertion for Epitope Mapping Method. *Monoclon Antib Immunodiagn Immunother* **2021**, *40*, 162-167, doi:10.1089/mab.2021.0023.
67. Nanamiya, R.; Sano, M.; Asano, T.; Yanaka, M.; Nakamura, T.; Saito, M.; Tanaka, T.; Hosono, H.; Tateyama, N.; Kaneko, M.K.; et al. Epitope Mapping of an Anti-Human Epidermal Growth Factor Receptor Monoclonal Antibody (EMab-51) Using the RIEDL Insertion for Epitope Mapping Method. *Monoclon Antib Immunodiagn Immunother* **2021**, *40*, 149-155, doi:10.1089/mab.2021.0010.
68. Spatola, B.N.; Lerner, A.G.; Wong, C.; Dela Cruz, T.; Welch, M.; Fung, W.; Kovalenko, M.; Losenkova, K.; Yegutkin, G.G.; Beers, C.; et al. Fully human anti-CD39 antibody potently inhibits ATPase activity in cancer cells via uncompetitive allosteric mechanism. *MAbs* **2020**, *12*, 1838036, doi:10.1080/19420862.2020.1838036.
69. Zhang, H.; Feng, L.; de Andrade Mello, P.; Mao, C.; Near, R.; Csizmadia, E.; Chan, L.L.; Enjyoji, K.; Gao, W.; Zhao, H.; et al. Glycoengineered anti-CD39 promotes anticancer responses by depleting suppressive cells and inhibiting angiogenesis in tumor models. *J Clin Invest* **2022**, *132*, doi:10.1172/jci157431.
70. Li, G.; Suzuki, H.; Ohishi, T.; Asano, T.; Tanaka, T.; Yanaka, M.; Nakamura, T.; Yoshikawa, T.; Kawada, M.; Kaneko, M.K.; et al. Antitumor activities of a defucosylated anti-EpCAM monoclonal antibody in colorectal carcinoma xenograft models. *Int J Mol Med* **2023**, *51*, doi:10.3892/ijmm.2023.5221.
71. Nanamiya, R.; Takei, J.; Ohishi, T.; Asano, T.; Tanaka, T.; Sano, M.; Nakamura, T.; Yanaka, M.; Handa, S.; Tateyama, N.; et al. Defucosylated Anti-Epidermal Growth Factor Receptor Monoclonal Antibody (134-mG(2a)-f) Exerts Antitumor Activities in Mouse Xenograft Models of Canine Osteosarcoma. *Monoclon Antib Immunodiagn Immunother* **2022**, *41*, 1-7, doi:10.1089/mab.2021.0036.
72. Kawabata, H.; Suzuki, H.; Ohishi, T.; Kawada, M.; Kaneko, M.K.; Kato, Y. A Defucosylated Mouse Anti-CD10 Monoclonal Antibody (31-mG(2a)-f) Exerts Antitumor Activity in a Mouse Xenograft Model of CD10-Overexpressed Tumors. *Monoclon Antib Immunodiagn Immunother* **2022**, *41*, 59-66, doi:10.1089/mab.2021.0048.
73. Kawabata, H.; Ohishi, T.; Suzuki, H.; Asano, T.; Kawada, M.; Suzuki, H.; Kaneko, M.K.; Kato, Y. A Defucosylated Mouse Anti-CD10 Monoclonal Antibody (31-mG(2a)-f) Exerts Antitumor Activity in a Mouse Xenograft Model of Renal Cell Cancers. *Monoclon Antib Immunodiagn Immunother* **2022**, doi:10.1089/mab.2021.0049.
74. Asano, T.; Tanaka, T.; Suzuki, H.; Li, G.; Ohishi, T.; Kawada, M.; Yoshikawa, T.; Kaneko, M.K.; Kato, Y. A Defucosylated Anti-EpCAM Monoclonal Antibody (EpMab-37-mG(2a)-f) Exerts Antitumor Activity in Xenograft Model. *Antibodies (Basel)* **2022**, *11*, doi:10.3390/antib11040074.
75. Tateyama, N.; Nanamiya, R.; Ohishi, T.; Takei, J.; Nakamura, T.; Yanaka, M.; Hosono, H.; Saito, M.; Asano, T.; Tanaka, T.; et al. Defucosylated Anti-Epidermal Growth Factor Receptor Monoclonal Antibody 134-mG(2a)-f Exerts Antitumor Activities in Mouse Xenograft Models of Dog Epidermal Growth Factor Receptor-Overexpressed Cells. *Monoclon Antib Immunodiagn Immunother* **2021**, *40*, 177-183, doi:10.1089/mab.2021.0022.
76. Takei, J.; Ohishi, T.; Kaneko, M.K.; Harada, H.; Kawada, M.; Kato, Y. A defucosylated anti-PD-L1 monoclonal antibody 13-mG(2a)-f exerts antitumor effects in mouse xenograft models of oral squamous cell carcinoma. *Biochem Biophys Rep* **2020**, *24*, 100801, doi:10.1016/j.bbrep.2020.100801.
77. Takei, J.; Kaneko, M.K.; Ohishi, T.; Hosono, H.; Nakamura, T.; Yanaka, M.; Sano, M.; Asano, T.; Sayama, Y.; Kawada, M.; et al. A defucosylated antiCD44 monoclonal antibody 5mG2af exerts antitumor effects in mouse xenograft models of oral squamous cell carcinoma. *Oncol Rep* **2020**, *44*, 1949-1960, doi:10.3892/or.2020.7735.